X-RAY DIFFRACTION

Jenő Gubicza

Department of Materials Physics, Eötvös Loránd University, Budapest, Hungary

Supported by the Higher Education Restructuring Fund allocated to ELTE by the Hungarian Government

1. INTRODUCTION

Wilhelm Conrad Röntgen discovered X-ray radiation in 1895 and recognized that its absorption depends on the mass density of materials. He received Nobel prize for his achievement in 1901. In the beginning of 20th century, the physicists suggested that X-ray is a form of electromagnetic radiation. For the justification of this supposition an interference experiment was necessary to perform on a periodic lattice with a similar period length as the suspected wavelength of X-rays (10^{-10} m). Assuming that crystalline materials have periodic lattice structure, Max von Laue calculated the conditions necessary for diffraction by X-rays. In 1912 according to Laue's calculations Friedrich and Knipping place a copper-sulphate single crystal in the path of X-rays and detected interference intensity spots on a film. With this experiment they established the fact that X-rays are electromagnetic in nature and opened the way to the investigation of the crystal structure by X-ray diffraction. Laue was awarded by Nobel prize in 1914. Since then, X-ray diffraction became a basic method of crystal structure determination in materials science. In this chapter, the theoretical background of powder diffraction and the basic evaluation methods of diffraction patterns are presented.

2. THEORETICAL BACKGROUND

2.1. KINEMATICAL THEORY OF DIFFRACTION

In the kinematical theory of diffraction it is assumed that (i) the scattering is elastic, i.e. the wavelength of X-ray photons does not change in the scattering event, (ii) the diffraction is coherent, which means that the phase change of the X-ray wave during scattering is the same for all

scattering events and (iii) each photon is scattered only once, i.e. the diffracted wave is not scattered again inside the crystal. The latter criterion is a realistic approximation if the scattered intensity is much weaker than the incident intensity [1]. Regarding the scattering mechanisms, when X-ray photons hit an atom, the center of gravity of the electron-cloud is moved away from the position of the nucleus. This electric dipole vibrates and radiates X-rays. With conditions (i)-(iii) the interference is determined solely by the positions of the scattering centers (electrons in the case of X-ray diffraction). As most electrons are located near the nuclei of atoms, the diffracted intensity distribution is mainly determined by the atomic arrangement in the crystal. This correlation enables the determination of the crystal structure from the position and intensity of the diffraction peaks.

First, let's investigate the interference of X-rays diffracted from two scattering centers (electrons) in a crystal. One of the scattering centers is selected for the origin of the coordinate system in the crystal (denoted by *O* in Fig. 1). The vector pointing to the second scattering center (point *P* in Fig. 1) is denoted by $\boldsymbol{r}$. The crystal is radiated by a monochromatic primary X-ray beam with the wave-vector $\boldsymbol{k}_o$ which represents the direction of the beam and its magnitude is the reciprocal of the wavelength, λ ($|\boldsymbol{k}_0| = 1/\lambda$). Since the scattering is elastic, the diffracted beam has the same wavelength as the primary radiation. The amplitude of X-rays scattered into the direction represented by the wave-vector $\boldsymbol{k}$ ($|\boldsymbol{k}| = 1/\lambda$) is determined by the difference in the paths of the beams diffracted from the two scattering centers. Considering that the distances of the source of X-rays and the point of observation (detector) from the sample crystal are both much larger than the spacings between the scattering centers inside the crystal ($|\boldsymbol{r}|$), the plane wave approximation can be used in the calculation of interference effects. Accordingly, Fig. 1 shows that the difference between the paths of the X-ray beams scattered from the two electrons is $(\boldsymbol{k}_o\text{-}\boldsymbol{k})\cdot\boldsymbol{r} = -\boldsymbol{\kappa}\boldsymbol{r}$, where $\boldsymbol{\kappa} = \boldsymbol{k}\text{-}\boldsymbol{k}_o$ is referred to as scattering vector. As a consequence, the scattered amplitude (A) is a function of $\boldsymbol{\kappa}$ which can be given by the following expression:

$$A(\boldsymbol{\kappa}) = A_0 \exp(-2\pi i \boldsymbol{\kappa}\boldsymbol{r}), \qquad (1)$$

where coefficient A_0 depends on the intensity of the primary beam and the strength of scattering (i.e. how much of the incident beam is scattered elastically). Since we investigate only the influence of spatial arrange-

ment of scattering centers on diffracted amplitude, and the value of Ψ_0 is the same for all scattering centers, therefore A_0 will be omitted in the following calculations. For the determination of the amplitude diffracted from the whole crystal, the amplitudes scattered from the individual electrons should be summed up. Introducing the electron density function $\rho(\boldsymbol{r})$ which gives the number of electrons in a unit volume at the position $\boldsymbol{r}$, the amplitude scattered from the whole crystal can be given as an integral over the volume of the crystal, V:

$$A(\boldsymbol{\kappa}) = \int_V \rho(\boldsymbol{r}) \exp(-2\pi i \boldsymbol{\kappa r}) dV \,. \qquad (2)$$

Eq. (2) suggests that the amplitude of the elastically scattered X-rays is proportional to the Fourier-transform of the electron density.

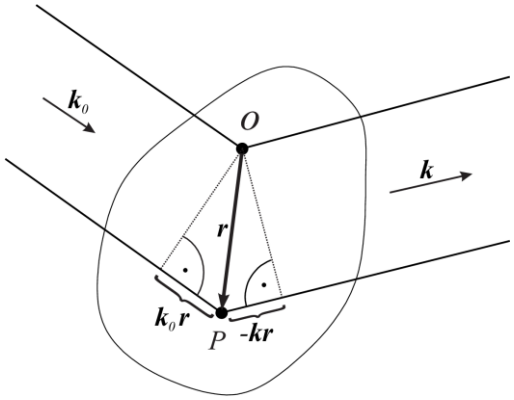

Figure 1: Plane wave approximation of X-ray diffraction in the case of two scattering centers [2].

The electron density follows the periodicity of the crystal, i.e.

$$\rho(\boldsymbol{r}) = \rho(\boldsymbol{r} + \boldsymbol{R_n}). \qquad (3)$$

$\boldsymbol{R_n}$ is an arbitrary lattice vector given as $\boldsymbol{R}_n = n_1\boldsymbol{a}_1 + n_2\boldsymbol{a}_2 + n_3\boldsymbol{a}_3$, where n_i are integers and $\boldsymbol{a_1}$, $\boldsymbol{a_2}$ and $\boldsymbol{a_3}$ are the unit vectors describing the lattice. Using eq. (3) the following formula is valid for the amplitude:

$$A(\boldsymbol{\kappa}) = \int_V \rho(\boldsymbol{r}) \exp(-2\pi i \boldsymbol{\kappa r}) dV = \int_V \rho(\boldsymbol{r} + \boldsymbol{R_n}) \exp(-2\pi i \boldsymbol{\kappa r}) dV \,. \quad (4)$$

Substituting $\boldsymbol{r}+\boldsymbol{R_n}$ by $\boldsymbol{r'}$ in the right side of eq. (4) we get:

$$\begin{aligned} A(\boldsymbol{\kappa}) &= \int_V \rho(\boldsymbol{r}')\exp(-2\pi i\boldsymbol{\kappa}(\boldsymbol{r}' - \boldsymbol{R}_n))dV \\ &= \exp(2\pi i\boldsymbol{\kappa}\boldsymbol{R}_n)\int_V \rho(\boldsymbol{r}')\exp(-2\pi i\boldsymbol{\kappa}\boldsymbol{r}')dV = \exp(2\pi i\boldsymbol{\kappa}\boldsymbol{R}_n)A(\boldsymbol{\kappa}) \end{aligned} \tag{5}$$

Eq. (5) suggests that in the directions where the amplitude is non-zero, the scattering vector, $\boldsymbol{\kappa}$ should obey the following equation for any lattice vector, $\boldsymbol{R_n}$:

$$\exp(2\pi i\boldsymbol{\kappa}\boldsymbol{R}_n) = 1. \tag{6}$$

Eq. (6) is fulfilled if the scalar product $\boldsymbol{\kappa}\cdot\boldsymbol{R_n}$ is an integer number for any lattice vector, $\boldsymbol{R_n}$. This condition is obeyed only if the scattering vector $\boldsymbol{\kappa}$ equals $h\cdot\boldsymbol{b}_1+k\cdot\boldsymbol{b}_2+l\cdot\boldsymbol{b}_3$, where h, k and l are integers and $\boldsymbol{a}_i\cdot\boldsymbol{b}_j=\delta_{ij}$, where δ_{ij} = 1 for $i = j$ and 0 for $i \neq j$ [1]. The last condition is fulfilled only if vectors $\boldsymbol{b}_1$, $\boldsymbol{b}_2$ and $\boldsymbol{b}_3$ are selected as:

$$\boldsymbol{b}_1 = \frac{\boldsymbol{a}_2 \times \boldsymbol{a}_3}{\boldsymbol{a}_1(\boldsymbol{a}_2 \times \boldsymbol{a}_3)}, \tag{7}$$

$$\boldsymbol{b}_2 = \frac{\boldsymbol{a}_3 \times \boldsymbol{a}_1}{\boldsymbol{a}_1(\boldsymbol{a}_2 \times \boldsymbol{a}_3)}, \tag{8}$$

$$\boldsymbol{b}_3 = \frac{\boldsymbol{a}_1 \times \boldsymbol{a}_2}{\boldsymbol{a}_1(\boldsymbol{a}_2 \times \boldsymbol{a}_3)}. \tag{9}$$

Considering $\boldsymbol{b}_1$, $\boldsymbol{b}_2$ and $\boldsymbol{b}_3$ as unit vectors, a lattice can be built up from them which is referred to as reciprocal lattice [3]. In the case of crystals with cubic structure, the reciprocal lattice is also cubic and the length of vector $\boldsymbol{b}_i$ is the reciprocal of the magnitude of the corresponding vector $\boldsymbol{a}_i$. The unit of the magnitude of $\boldsymbol{b}_i$ is one over length. As the unit of the scattering vector $\boldsymbol{\kappa}$ is also one over length, it can be regarded as a vector in the reciprocal space. According to the considerations presented above, a maximum is obtained in the scattered intensity for the direction represented by $\boldsymbol{k}$ if the following condition is fulfilled:

$$\boldsymbol{k} - \boldsymbol{k}_0 = \boldsymbol{g}_{hkl}\,, \tag{10}$$

where $\boldsymbol{g}_{hkl}$ is a reciprocal lattice vector ($\boldsymbol{g}_{hkl}=h\cdot\boldsymbol{b}_1+k\cdot\boldsymbol{b}_2+l\cdot\boldsymbol{b}_3$). Another and equivalent wording of this condition says that if the reciprocal space vector $\boldsymbol{\kappa}$ determined by the wave-vectors of the primary ($\boldsymbol{k}_0$) and diffracted ($\boldsymbol{k}$) beams matches with a reciprocal lattice vector $\boldsymbol{g}_{hkl}$, an intensity maximum in the scattered intensity is obtained.

Taking into account the periodicity of the crystal lattice and assuming that the electron density ρ is the sum of the electron densities of the atoms in the unit cell, the amplitude can be written as [1]:

$$A(\boldsymbol{\kappa}) = \sum_n \left\{ \int_{V_c} \left[\sum_p \rho_p \exp(-2\pi\boldsymbol{\kappa}\boldsymbol{r}) \right] dV \right\}, \tag{11}$$

where ρ_p is the electron density for p^{th} atom in the cell and the values of n are the indices of the cells in the crystal. Let us write the position vector of an electron as $\boldsymbol{r} = \boldsymbol{R}_n+\boldsymbol{r}_p+\boldsymbol{r'}$ where $\boldsymbol{R}_n$ is the lattice vector pointing from the origin of the lattice to the corner of the n^{th} cell, $\boldsymbol{r}_p$ is the position vector of the p^{th} atom inside the n^{th} cell and $\boldsymbol{r'}$ gives the position of the electron around the p^{th} atom (see Fig. 2). Then, eq. (11) can be reformulated as:

$$A(\boldsymbol{\kappa}) = \sum_n \left\{ \sum_p \left[\int_{V_c} \rho_p \exp(-2\pi\boldsymbol{\kappa}\boldsymbol{r}') \right] \exp(-2\pi\boldsymbol{\kappa}\boldsymbol{r}_p) \right\} \exp(-2\pi i\boldsymbol{\kappa}\boldsymbol{R}_n). \tag{12}$$

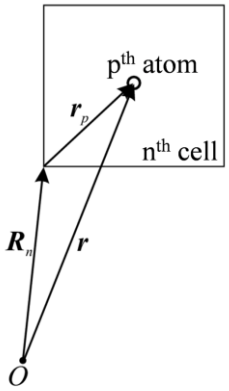

Figure 2. Subdivision of a position vector pointing to the p^{th} atom in the n^{th} lattice cell [2].

The expression inside the square brackets reflects the scattering of electrons for the p^{th} atom in the cell, therefore it is referred to as atomic scattering factor or atomic form factor and denoted by f_p

$$f_p = \int_{V_c} \rho_p \exp(-2\pi \boldsymbol{\kappa} \boldsymbol{r}'). \tag{13}$$

The value of f_p depends on the type of atom and the scattering angle. The term in the braces of eq. (12) describes the scattering of a cell in the crystal, therefore it is referred to as structure factor and denoted by F:

$$F(\boldsymbol{\kappa}) = \sum_p f_p \exp(-2\pi \boldsymbol{\kappa} \boldsymbol{r_p}). \tag{14}$$

F depends on the types and positions of the atoms in the cell, as well as the scattering angle. Finally, the scattered amplitude can be given as:

$$A(\boldsymbol{\kappa}) = F(\boldsymbol{\kappa}) \sum_n \exp(-2\pi i \boldsymbol{\kappa} \boldsymbol{R_n}). \tag{15}$$

The intensity of the scattered X-rays in the center of the diffraction peak (i.e. if $\boldsymbol{\kappa} = \boldsymbol{g}_{hkl}$) is given as:

$$I(\boldsymbol{g}_{hkl}) = |A(\boldsymbol{g}_{hkl})|^2 = |F(\boldsymbol{g}_{hkl})|^2 \left| \sum_n \exp(-2\pi i \boldsymbol{g}_{hkl} \boldsymbol{R}_n) \right|^2 = |F(\boldsymbol{g}_{hkl})|^2 N^2, \tag{16}$$

where N is the number of cells in the crystal volume.

2.2. CORRELATION BETWEEN THE CRYSTAL LATTICE PLANES AND THE RECIPROCAL LATTICE VECTORS

A family of crystal lattice planes (a set of parallel equidistant lattice planes) can be identified by three integers referred to as Miller indices. In order to determine the Miller indices for a plane family, let's take a coordinate system with three axes parallel to the unit vectors of the lattice and place the origin of the system at a lattice point on one of the set of planes (denoted by O in Fig. 3). The next nearest plane makes intersections A, B and C with the three crystallographic axes parallel to the unit vectors $\boldsymbol{a}_1$,

$\boldsymbol{a}_2$ and $\boldsymbol{a}_3$, respectively. Due to the translational symmetry of the crystal, the number of lattice planes intersecting any section connecting two neighboring lattice points can only be an integer number. Therefore, the sections *OA*, *OB* and *OC* can be expressed as $\boldsymbol{a}_1/h$, $\boldsymbol{a}_2/k$ and $\boldsymbol{a}_3/l$, respectively, where *h*, *k* and *l* are integers [4]. The (*hkl*) numbers identifying the family of planes is referred to as Miller indices.

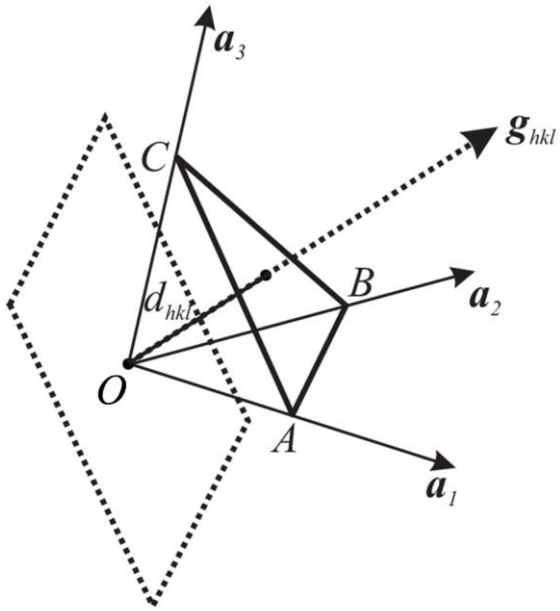

Figure 3. Intersection of a lattice plane family with the three axes of the crystal lattice [2].

For a crystal there is a direct correspondence between the families of lattice planes and the reciprocal lattice vectors. Namely, the reciprocal lattice vector $\boldsymbol{g}_{hkl}$ is perpendicular to the lattice planes with the Miller indices (*hkl*) and the reciprocal of the magnitude of $\boldsymbol{g}_{hkl}$ equals the interplanar spacing of these planes. The former statement can be easily proved by taking the scalar product of vector $\boldsymbol{g}_{\boldsymbol{hkl}}$ and the vector ($\boldsymbol{a}_1/h$-$\boldsymbol{a}_2/k$) corresponding to section *BA* in plane (*hkl*). This product is zero since $\boldsymbol{a}_i \cdot \boldsymbol{b}_j = \delta_{ij}$ which indicates that the two vectors are perpendicular. Due to the same reasons vector $\boldsymbol{g}_{\boldsymbol{hkl}}$ is perpendicular to vectors ($\boldsymbol{a}_2/k$-$\boldsymbol{a}_3/l$) and ($\boldsymbol{a}_3/l$-$\boldsymbol{a}_1/h$). If vector $\boldsymbol{g}_{\boldsymbol{hkl}}$ is perpendicular to two vectors in plane (*hkl*), it is perpendicular to the plane. The interplanar spacing for planes (*hkl*) denoted by d_{hkl} can be obtained as the distance between the origin *O* and the plane *ABC* in Fig. 3. This distance is calculated as the projection of vector $\boldsymbol{a}_1/h$ nor-

mal to planes (*hkl*), which can be determined as the scalar product of this vector and the unit vector parallel to $\boldsymbol{g}_{hkl}$:

$$d_{hkl} = \frac{\boldsymbol{a}_1}{h}\frac{\boldsymbol{g}_{hkl}}{|\boldsymbol{g}_{hkl}|} = \frac{\boldsymbol{a}_1}{h}\frac{h\boldsymbol{b}_1 + k\boldsymbol{b}_2 + l\boldsymbol{b}_3}{|\boldsymbol{g}_{hkl}|} = \frac{1}{|\boldsymbol{g}_{hkl}|}. \qquad (17)$$

It should be noted that not all reciprocal lattice vectors correspond to real lattice planes in the crystal. For instance, let's select the lattice planes with the Miller indices (*hkl*) which related to the reciprocal vector $\boldsymbol{g}_{hkl}$. The interplanar spacing for this plane family is $d_{hkl} = 1/|\boldsymbol{g}_{hkl}|$. The vectors $m\cdot\boldsymbol{g}_{hkl}$ (*m* are integers) are also reciprocal lattice vectors and the spacing between the corresponding lattice planes is d_{hkl}/m. As the distance between the neighboring planes perpendicular to vector $\boldsymbol{g}_{hkl}$ is d_{hkl}, therefore the planes (*mh,mk,ml*) are not real but rather fictive lattice planes in the crystal (there are no lattice points on them). It is noted that the real and the fictive lattice planes are not distinguished in X-ray diffraction studies [5].

2.3. EWALD CONSTRUCTION

The Ewald construction is the graphical representation of the condition obtained for the diffraction intensity maxima and given by eq. (10) [1]. The Ewald construction is illustrated in Fig. 4 where the reciprocal lattice points are represented by black solid circles. The wave-vector of the incident (or primary) radiation, $\boldsymbol{k}_o$ terminates on the origin of the reciprocal lattice (point *O* in Fig. 4). Let's draw a sphere with a radius of $1/\lambda$ which is centered on the intial end of vector $\boldsymbol{k}_o$. This sphere referred to as Ewald sphere passes through the origin of the reciprocal lattice. If a reciprocal point with the indices of *hkl* falls on the surface of the sphere, it represents a diffraction maximum for which the diffraction condition $\boldsymbol{k} - \boldsymbol{k}_0 = \boldsymbol{g}_{hkl}$ is fulfilled. The direction of the maximum diffracted intensity is given by the wave-vector $\boldsymbol{k}$ which starts in the origin of the Ewald sphere and ends at the reciprocal lattice point *hkl* (see Fig. 4). As the scattering is elastic, both $\boldsymbol{k}$ and $\boldsymbol{k}_o$ vectors have the magnitude of $1/\lambda$. The difference between the vectors $\boldsymbol{k}$ and $\boldsymbol{k}_o$ gives $\boldsymbol{g}_{hkl}$ as shown in Fig. 4 in agreement with the diffraction condition presented in eq. (10). The diffraction peak corresponds to the reciprocal lattice point *hkl* can also be denoted by the same three indices. If the relative orientation of the crystal and the primary monochromatic beam is fixed, most probably only a few

reciprocal points fall on the surface of the Ewald sphere. Therefore, the diffraction maxima corresponding to other reciprocal points are not detected in the experiment. If the crystal is rotated during measurement, the reciprocal lattice is also turned around its origin *O*. As a consequence, in the experiment all the diffraction maxima can be obtained for which the magnitude of the reciprocal vector is smaller than the diameter of the Ewald sphere, i.e. $|\boldsymbol{g}_{hkl}| \leq 2/\lambda$. It is noted that the reciprocal vector $\boldsymbol{g}_{hkl}$ is also referred to as the diffraction vector for peak *hkl*.

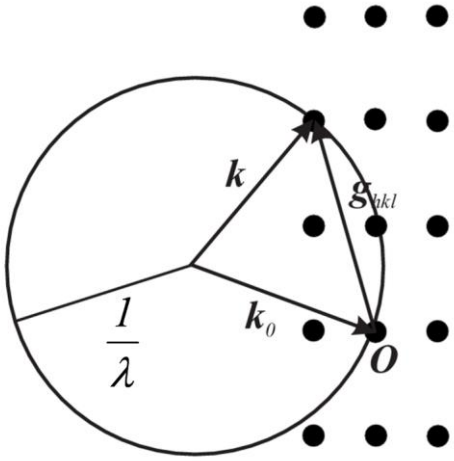

Figure 4. Ewald construction [2].

In the case of powder or untextured polycrystalline materials, the crystallites have random crystallographic orientation. Therefore, the reciprocal lattice is rotated around its origin *O* and in the Ewald construction the *hkl* reciprocal lattice point is substituted by a sphere which is centered at point *O* and has the radius $|\boldsymbol{g}_{hkl}|$ (see Fig. 5). The common circle of sphere *hkl* and the Ewald sphere gives the directions of the diffracted beams. Consequently, all the diffraction peaks are detected in the experiment for which $|\boldsymbol{g}_{hkl}| \leq 2/\lambda$ irrespectively of the sample orientation relative to the primary beam.

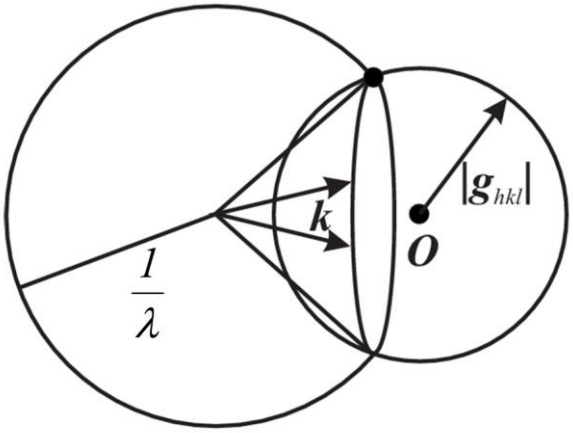

Figure 5. Ewald construction for polycrystalline material consisting of crystallites with random crystallographic orientation [2].

2.4. BRAGG'S LAW

Using the relationship between the reciprocal lattice vectors and the crystal lattice planes, the diffraction condition in eq. (10) can be expressed in terms of the interplanar spacings. Fig. 6 shows that the difference between the vectors $\boldsymbol{k}$ and $\boldsymbol{k}_o$ gives $\boldsymbol{g}_{hkl}$. The magnitude of both vectors $\boldsymbol{k}$ and $\boldsymbol{k}_o$ is $1/\lambda$ while the length of vector $\boldsymbol{g}_{hkl}$ is $1/d_{hkl}$. Therefore, in triangle EFG the following equation holds [1-4]:

$$2d_{hkl}\sin\theta = \lambda\,, \tag{18}$$

where θ is the half of the angle between vectors $\boldsymbol{k}$ and $\boldsymbol{k}_o$. Eq. (18) enables to calculate the angles between the directions of the diffracted maxima and the incident beam (2θ) from the wavelength of X-rays (λ) and the interplanar spacings (d_{hkl}). For monochromatic X-ray radiation each lattice plane family is related to a diffraction maximum. Condition $|\boldsymbol{g}_{hkl}| \le 2/\lambda$ discussed above is equivalent to $d_{hkl} \ge \lambda/2$ which limits the number of plane families contributing to the diffraction pattern.

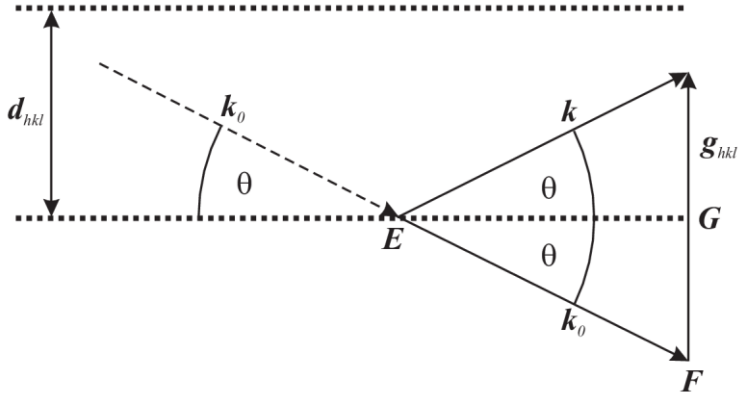

*Figure 6. Relation between the wave vectors (**k**$_0$ and **k**), the reflecting lattice planes (indicated by dotted lines) and the corresponding reciprocal lattice vector (**g**$_{hkl}$) when the diffraction condition in eq. (10) is fulfilled [2].*

In Fig. 6 two planes in the family (*hkl*) are indicated by dotted lines which are perpendicular to the diffraction vector $\boldsymbol{g}_{hkl}$ and their interplanar spacing is d_{hkl}. If the intial end of vector $\boldsymbol{k}_o$ is placed in point E (indicated by dashed arrow), the layout of $\boldsymbol{k}_o$, $\boldsymbol{k}$ and plane EG suggests that X-ray diffraction can be handled as reflection of X-rays by lattice planes [3]. The reflection rules used in optics can also be applied here: (i) the angle of incidence agrees with the reflection angle (both are θ) and (ii) diffraction maxima are obtained if the difference between the paths of beams reflected from different members of a plane family is an integer multiple of the wavelength. These conditions are equivalent to eq. (18) which is referred to as Bragg's law after its creators W. L. Bragg and his father W. H. Bragg. They were awarded by Nobel prize in 1915. The diffraction peaks are also referred to as Bragg reflections and the angle θ is often called as Bragg angle. Eqs. (10) and (18), as well as the Ewald construction are equivalent formulations of the condition for scattered intensity maxima.

2.5. STRUCTURE FACTOR AND SYSTEMATIC EXTINCTION

Eq. (16) shows that the intensity of a diffraction peak is proportional to the square of the structure factor. Substituting $\boldsymbol{\kappa} = \boldsymbol{g}_{hkl} = h\cdot\boldsymbol{b}_1+k\cdot\boldsymbol{b}_2+l\cdot\boldsymbol{b}_3$ and $\boldsymbol{r}_p=x_p\cdot\boldsymbol{a}_1+y_p\cdot\boldsymbol{a}_2+z_p\cdot\boldsymbol{a}_3$ into eq. (14), the following formula is obtained for the structure factor:

$$F(hkl)=\sum_p f_p e^{-2\pi i\left(hx_p+ky_p+lz_p\right)}. \qquad (19)$$

Due to the symmetry properties of the crystal structure, the structure factor becomes zero for some *hkl* reflections and therefore the corresponding peaks do not appear in the diffractogram. This phenomenon is referred to as *systematic extinction*. In the following paragraphs we investigate this effect for body-centered cubic (*bcc*) and face-centered cubic (*fcc*) structures. For the simplicity let's assume that there is only one atom in each lattice point.

For a *bcc* structure there are two lattice points in the Bravais cell with the following coordinates: (*0,0,0*) and (*1/2,1/2,1/2*). Accordingly, the structure factor is given as:

$$F(hkl)=f\left(e^{-2\pi i(0+0+0)}+e^{-\pi i(h+k+l)}\right)=f\left(1+(-1)^{h+k+l}\right) \qquad (20)$$

Thus, $F(hkl)=2f$, if $h+k+l$ is an even number, and $F(hkl)=0$, if $h+k+l$ is odd. Therefore, in the case of a *bcc* structure only those reflections appear in the diffractogram for which $h+k+l$ is even.

For an *fcc* structure there are four lattice points in the Bravais cell with the following coordinates:: (*0,0,0*), (*1/2,1/2,0*), (*1/2,0,1/2*) and (*0,1/2,1/2*). Thus, the structure factor can be given as:

$$\begin{aligned} F(hkl) &= f\left(e^{-2\pi i(0+0+0)}+e^{-\pi i(h+k)}+e^{-\pi i(h+l)}+e^{-\pi i(l+k)}\right) \\ &= f\left(1+(-1)^{h+k}+(-1)^{h+l}+(-1)^{l+k}\right) \end{aligned} \qquad (21)$$

$F(hkl)=4f$, if all the three indices *h*, *k*, *l* are even or odd, and $F(hkl)=0$, if *h*, *k*, *l* are mixed. Therefore, for *fcc* structures only those reflections appear in the diffractograms which have indices with the same parities.

A lattice point may contain more than one atom. The atom or the group of atoms (e.g. a molecule) occupying the lattice point is called as *basis*. In the case of a diamond cubic lattice, the lattice points form an *fcc* structure and the basis consists of two identical atoms with the following coordinates in the Bravais cell: (*0,0,0*) and (*1/4,1/4,1/4*). In other words, the diamond cubic lattice consists of two identical interpenetrating *fcc* sublattices displaced along the body diagonal of the cubic Bravais cell by ¼th length of that diagonal. The calculation of the structure factor for diamond cubic structure reveals that the extinction rule for *fcc* structure also holds here, but in addition those *fcc* reflections disappear from the

diffractogram for which $h^2+k^2+l^2 = 4\cdot(2j+1)$, where j is an integer number.

The positions (2θ angles) and the relative intensities of the diffractions peaks in diffractograms can be used for the determination of the crystal structure. In the next sections, some evaluation methods of X-ray powder (or polycrystalline) diffractograms are described.

3. METHODS FOR THE EVALUATION OF POWDER DIFFRACTION PATTERNS

3.1. POWDER DIFFRACTION PATTERN

In powder diffraction experiments the volume irradiated by X-rays contains a large number of randomly orientated crystallites. In this case the scattered intensity distribution around the sample does not depend on the orientation of the sample relative to the incident beam. In a powder diffraction experiment the scattered intensity is measured as a function of 2θ. As an example, Fig. 7 shows a powder pattern obtained on an *fcc* aluminum. Each peak corresponds to a lattice plane family, therefore the indices of the peaks are the same as the indices of the corresponding lattice planes. The 2θ angle values of the peaks can be calculated from the interplanar spacings d_{hkl} using the Bragg equation (see eq. (18)). The area under the peaks is referred to as integrated intensity. In the calculation of the integrated intensity, A_o in eq. (1) have to be taken into account and the integration in eq. (2) should be carry out for the whole illuminated volume. Finally, the following formula is obtained for the integrated intensity of peak *hkl* [1]:

$$I = I' m_{hkl} \left|F(hkl)\right|^2 e^{-2M} LP\,, \tag{22}$$

where I' depends on the intensity of the incident beam, the distance between the sample and the detector, the irradiated volume, the sample absorption and the wavelength of X-rays. Factor I' is the same for all reflections in a diffraction pattern, and the difference between the peak intensities is caused by the other four factors. Factor m_{hkl} is referred to as *multiplicity* which gives the number of plane families with different Miller-indices which have the same spacing d_{hkl} and therefore reflect X-rays into the same Bragg angle θ. For instance, for an *fcc* lattice the intensity in reflection *200* is the sum of the intensities reflected from six different lattice plane families (*200*), ($\bar{2}00$), (*020*), ($0\bar{2}0$), (*002*), ($00\bar{2}$), where the

dash above the numbers indicates a minus sign. Therefore, the multiplicity for reflection *200* is six. The third factor in eq. (22) is the square of the structure factor. Its effect on the intensity was discussed in the former sections. The atoms and ions in the crystal lattice points vibrate around their ideal (equilibrium) positions. This thermal vibration results in a decrease of the peak intensity which is taken into account by the *Debye–Waller-factor* (the fourth term in eq. (22)). This effect becomes stronger with increasing the value of θ. The fifth factor in eq. (22) is referred to as *Lorentz-polarization factor* (*LP*), which depends on the diffraction angle as $(1+\cos^2\theta)/(\sin\theta\cdot\sin 2\theta)$ for the powder diffractometer described in the next section. Therefore, factor LP first reduces the peak intensity with increasing θ, however for large diffraction angles this factor yields an increase in intensity.

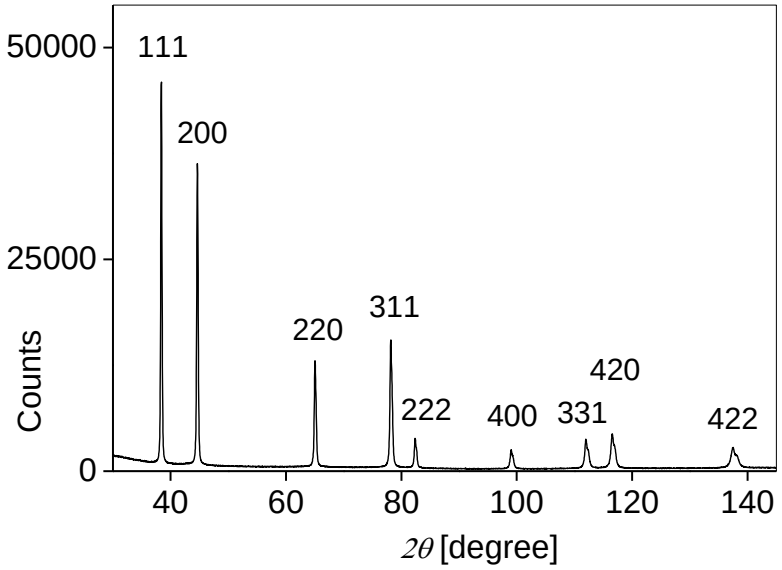

Figure 7. Powder diffraction pattern for an fcc Al sample [2].

3.1.1. POWDER DIFFRACTOMETER SETUP USED IN THE EXERCISES

The powder diffractometer used during the laboratory exercises is shown schematically in Fig. 8 [2].

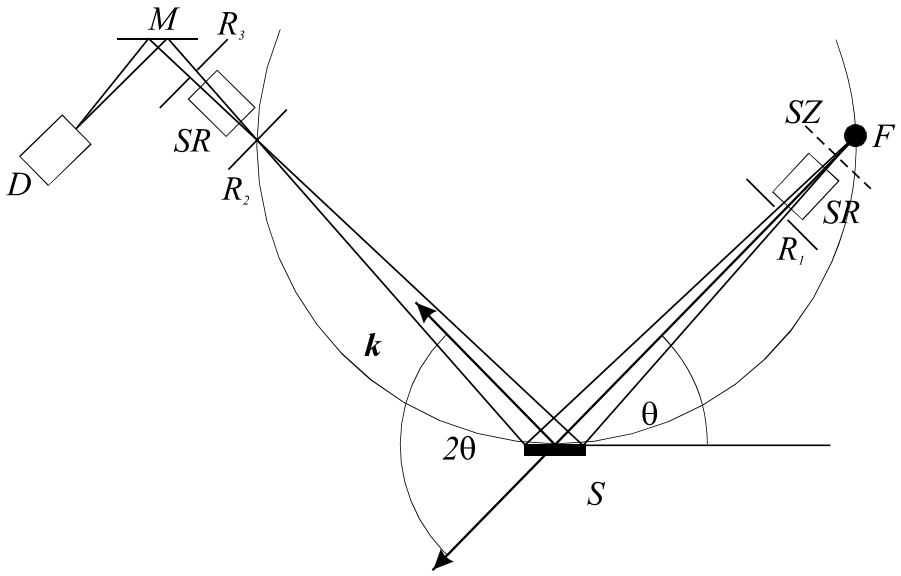

Figure 8. Powder diffractometer setup. F – X-ray source, SZ– filter, SR– Soller-slit, S – sample, R_1, R_2, R_3 – slits, M – monochromator, D – detector [2].

The source of X-ray radiation (also referred to as focus) is at the anod of a conventional X-ray tube and denoted by *F* in Fig. 8. The cathode (tungsten filament) of the tube emits electrons which are accelerated by the high voltage in the vacuum tube and collide to the anode. During collision a braking radiation (Bremsstrahlung) with continuous spectrum (white radiation) is produced. In addition, high intensity radiation with well defined wavelengths is also obtained. The wavelengths of this radiation are characteristic to the anode material, therefore it is referred to as *characteristic radiation*. Figure 9 shows a schematic spectrum of an X-ray tube. The bombarding electrons knock out electrons from the inner shells of the target atoms in the anode material. Then, the empty states are filled with electrons from outer shells. The $K\beta$ component of the characteristic radiation corresponds to the X-ray photons formed due to the transition of electrons from *M* shell to *K* shell. The characteristic peak $K\alpha$ in the spectrum is due to $L \rightarrow K$ electron transition. This line is actually a doublet containing two close peaks $K\alpha_1$ and $K\alpha_2$ with slightly different energies. The material of the anode is copper (*Cu*) in the diffractometer used in the laboratory exercises.

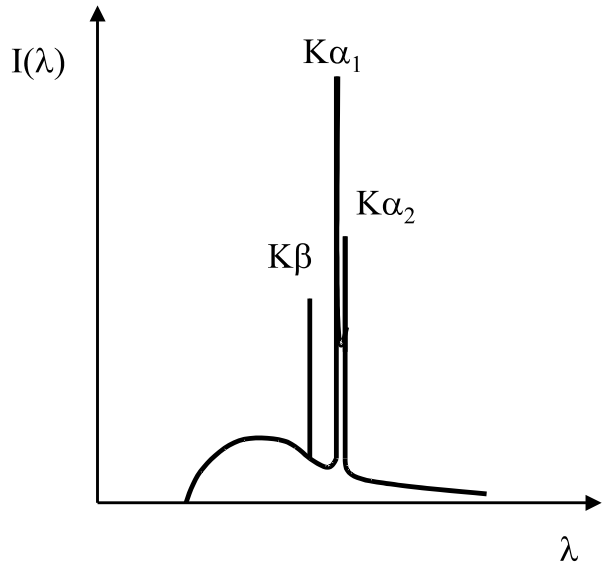

Figure 9. Schematic of an X-ray tube spectrum. λ and I denote the intensity and the wavelength, respectively [2].

The incidence beam leaving the tube has a divergence which is controlled parallel and perpendicular to the plane of Fig. 8 by slits R_1 and R_3, and the Soller-slit (*SR*), respectively. The latter slit consists of thin, parallel metallic plates. During the measurement the sample (*S*) and the detector (*D*) rotate around the axis going through the center of the sample perpendicular to the plane of Fig. 8. Slit R_2 attached to the detector and the X-ray source have the same distances from the sample. In the plane of Fig. 8 the circle going through slit R_2, the focus (*F*) and the center of the sample is referred to as focusing circle. The intersection of this circle and the sample is an arc. The X-ray beams reflected from the tangential crystalline planes at the points of this arc meet at slit R_2 due to the same scattering angle 2θ. Therefore, the intensity of the Bragg reflections is the highest if the sample always fits to the focusing circle during the measurement of the whole pattern. This can be achieved by rotating the sample to angle θ relative to the incident beam when the detector is at the diffraction angle 2θ (see Fig. 8). This configuration is referred to as θ-2θ diffractometer (or Bragg-Brentano diffraction geometry). It is noted that the focusing circle varies with the scattering angle 2θ.

During measurements the angular velocity of detector is twice the angular velocity of sample. The detector moves around the sample and detects the X-ray photons scattered into different diffraction angles 2θ.

The angle between the incident beam and the sample is the same as the angle between the sample and the detected scattered beam (symmetrical beam geometry). In a θ-2θ diffractometer the detector measures those scattered beams which are reflected from the lattice planes lying approximately parallel to the sample surface. For a non-textured polycrystalline sample all possible reflections appear in the powder diffraction pattern. In order to get only one reflection from one lattice plane family, the X-ray beam should be monochromatic, i.e. all detected X-ray photons must have the same wavelength. Figure 9 reveals that the highest scattered intensity is received if the wavelength of $CuK\alpha$ characteristic radiation is selected for the experiment from the spectrum of the X-ray tube. The unwanted radiation can be removed from the beam by a filter and a monochromator denoted by *SZ* and *M*, respectively, in Fig. 8. The filter is a thin foil which is made of the element whose atomic number is one less than that of the anode material. For instance, for *Cu* ande the filter material is *Ni*. The filter is placed immediately after the X-ray tube, therefore the incident beam at the sample does not contain component $K\beta$ of the radiation. In the diffractometer shown in Fig. 8 a *secondary* monochromator made of grafite crystal is also applied which can be found at the detector therefore it filters the beam scattered from the sample. The angle between the monochromator crystal and the scattered beam is adjusted according to the Bragg-equation in order to reflect only the $CuK\alpha$ radiation to the detector. The monochromator filters the radiation scattered non-elastically from the sample (e.g. fluorescent photons, Compton-scattering), thereby reducing the background. The detector used in our diffractometer is a proportional counter operated with Ar/methane gas mixture. An incoming X-ray photon results in an ionization of the Ar gas, thereby yielding an electric pulse. These pulses are collected as a function of the diffraction angle. The control of the measurement and the data collection are carried out by a computer. In the data collector softwer we can specify the starting and end 2θ angles, the step size of the detector motion and the measuring time between two steps. Finally, the counts as a function of 2θ are saved in a data file which can be evaluated by the methods described in the next sections.

3.1.2. EVALUATION OF POWDER DIFFRACTION PATTERNS

In the evaluation of a powder diffraction pattern, first the Bragg-angles of the diffraction peaks are determined. The Bragg-angle can be obtained directly by measuring the angle 2θ at the peak maximum or

indirectly by determining the center of an analytical function (e.g. Gaussian or Lorentzian) fitted to the measured data. Then, the interplanar spacing d_{hkl} is determined from the Bragg-equation using the wavelength λ of the monochromatized X-rays. If the incident X-ray beam is well monochromatized, and only radiation $K\alpha_1$ illuminates the sample, the angle θ at the peak maximum and the wavelength $\lambda_{K\alpha 1}$ are substituted into the Bragg-equation.

In the diffractometer used for the present laboratory exercises the monochromator is not able to eliminate $K\alpha_2$ radiation. Therefore, X-ray photons with two different wavelength corresponding to $K\alpha_1$ and $K\alpha_2$ radiations are detected. As a consequence, for each interplanar spacing d_{hkl} two reflections are observed. As $K\alpha_1$ and $K\alpha_2$ radiations have close wavelength values each diffraction peak consists of two close and overlapping reflections. The reflection appearing at lower angle corresponds to $K\alpha_1$ radiation due to the smaller wavelength compared to $K\alpha_2$ radiation. In the diffractogram the difference between the positions of $K\alpha_1$ and $K\alpha_2$ peaks increases with increasing angle 2θ. For small Bragg-angles the two peaks are not well separated and only an asymmetric reflection is observed. As in this case the Bragg-angle for $K\alpha_1$ radiation cannot be determined properly, the diffraction angle corresponding to the center of gravity of $K\alpha_1/K\alpha_2$ peak pair is determined. Then, d_{hkl} is calculated from the Bragg-equation using this angle and the weighted $K\alpha$ wavelength (denoted as $\lambda_{K\alpha}$) which can be calculated as:

$$\lambda_{K\alpha} = \frac{2\lambda_{K\alpha_1} + \lambda_{K\alpha_2}}{3}, \qquad (23)$$

where $\lambda_{K\alpha 1}=1.5405$ Å and $\lambda_{K\alpha 2}=1.5444$ Å. In eq. (23) the weights of $K\alpha_1$ and $K\alpha_2$ peaks are two and one, respectively, since the number of $K\alpha_1$ photons is twice the number of $K\alpha_2$ photons. Substituting, the values of $\lambda_{K\alpha 1}$ and $\lambda_{K\alpha 2}$ into eq. (23), 1.5418 Å is obtained for $\lambda_{K\alpha}$. After the d_{hkl} values for all measured reflections are determined, the unknown crystalline structure (also referred to as phase) can be identified by searching in a database or by indexing the diffraction peaks, as described in the next sections.

3.1.3. IDENTIFICATION OF CRYSTALLINE PHASES USING DATABASE

The positions and the relative intensities of diffraction peaks in the powder pattern for a randomly orientated polycrystalline material are determined by the structure of the crystal lattice and the type of atoms in the lattice points. Therefore, different crystalline materials yield different powder diffractograms, i.e. the diffraction pattern is a fingerprint of the crystalline phase. Since the first diffraction experiment performed in 1912, powder diffractograms for a large number of crystalline phases were determined and collected in databases. One of the most important databases is the *Powder Diffraction Files (ICDD-PDF)* which was made by the *International Centre for Diffraction Data (ICDD)* [6]. The latest issue of this database (*PDF-4+*) released in 2015 contains diffraction data for more than 365,000 crystalline materials. In the laboratory exercises an older version of ICDD-PDF database is used which contains 77,000 entries (also referred to as *cards*).

The crystalline phases in a studied material can be identified by comparing the experimentally determined powder pattern with the diffraction data in a database. In this search/match method different search criteria can be given which may be connected by logical operators (AND, OR). The most important criterion is based on the d_{hkl} values of the three strongest peaks in the pattern. The interplanar spacing values can be determined from the Bragg-angles of the three highest reflections using the Bragg-equation. Taking the uncertainty of peak positions into account, a range for d_{hkl} can be given for each reflection in the search software. These criteria for the three strongest peaks are connected by AND operator. Then, the search program selects those phases for which the three highest reflections can be found in the given ranges. If there is a phase among the selected ones for which the positions and the relative intensities of the other peaks also match with the experimentally measured reflections, the unknown phase is identified. Slight deviations between the peak positions and intensities in the diffraction patterns determined experimenally and found in the database can be accepted due to uncertainty of the measurement, as well as possible contaminations and crystallographic texture in the studied material. If the search performed on the basis of the peak positions and intensities yielded more than one candidates for the unknown phase, the search can be refined by additional criteria, e.g. by specifying chemical elements in the studied material.

3.1.4. INDEXING OF DIFFRACTION PATTERNS

If database is not available or the search yields no result, the crystal lattice can be identified by the process referred to as *peak indexing*. In this method the indices of reflections (*hkl*) in the powder pattern are determined. First, the values of d_{hkl} are calculated from the Bragg-angles of the peaks. Then, the values of $1/d_{hkl}^2$ are determined for all reflections. Due to the relationship $g_{hkl}^2 = 1/d_{hkl}^2$, the reciprocal of the square of interplanar spacing can be expressed with the reflection indices as [2]:

$$\frac{1}{d_{hkl}^2} = h^2A + k^2B + l^2C + 2hkD + 2klE + 2hlF\,, \tag{24}$$

where parameters *A, B,..., F* are positive and depend on the size and shape of unit cell. For cubic crystals eq. (24) is simplified as:

$$\frac{1}{d_{hkl}^2} = \frac{h^2 + k^2 + l^2}{a^2}\,, \tag{25}$$

where *a* is the lattice constant. Therefore, the values of $1/d_{hkl}^2$ for a cubic crystal can be expressed as $N(1/a^2)$, where $N = h^2+k^2+l^2$ are integer values. However, there are integer numbers which cannot be obtained as the sum of squares of three integers (e.g. *7, 15, 23, 28*), thus no peaks are related to these numbers. In general, these numbers can be obtained as $N=4^m(8n-1)$ where *n* and *m* are positive and negative integers [2]. There are additional *N* numbers for which reflections do not appear in the pattern due to systematic extinction. Table 1 shows the indices of the peaks appearing in the powder patterns for simple cubic, bcc, fcc and diamond cubic structures. In the first column of the table the sum of squares of peak indices is shown (*N*). In the second column the indices *hkl* are listed. Some *N* values can be obtained from essentially different indices *hkl* (they are not permutations) which is also indicated in the second column. The peaks appearing in the diffractograms for simple cubic, bcc, fcc and diamond cubic structures are marked by „x" in the last four columns of Table 1. For simple cubic structure peaks are obtained for all *N* integers which can be obtained as the sum of squares of three integers. For other cubic structures the number of reflections is lower due to systematic extinction.

Since the series of *N* values is different for the four cubic structures, the experimental values of *N* can be used for the identification of the

cubic lattice type. In practice, the values of *N* can be determined by dividing $1/d_{hkl}^2$ by $1/a^2$ (see eq. (25)). As the value of $1/a^2$ is unknown, we can try to find a value for $1/a^2$ which yields a series of integer numbers after the division that matches the *N* number series for a cubic lattice in Table 1. If we know which the first peak of the unknown phase is in the pattern, its *N* value have to be *1*, *2* or *3* (see Table 1). In this case, the series of $1/d_{hkl}^2$ is worth to divide by a value which results in *1*, *2* or *3* for the first peak. Then, the *N* numbers obtained for the other peaks can be compared with the series characteristic for the different cubic lattices.

N	*hkl*	Simple cubic	bcc	fcc	Diamond cubic
1	*100*	x			
2	*110*	x	x		
3	*111*	x		x	x
4	*200*	x	x	x	
5	*210*	x			
6	*211*	x	x		
(7)					
8	*220*	x	x	x	x
9	*300, 221*	x			
10	*310*	x	x		
11	*311*	x		x	x
12	*222*	x	x	x	
13	*320*	x			
14	*321*	x	x		
(15)					
16	*400*	x	x	x	x
17	*410, 322*	x			
18	*411, 330*	x	x		
19	*331*	x		x	x
20	*420*	x	x	x	
21	*421*	x			
22	*332*	x	x		
(23)					
24	*422*	x	x	x	x

Table 1. The indices of reflections hkl appeared in powder diffraction patterns for the four cubic structures (denoted by „x"). $N = h^2+k^2+l^2$ [2].

If our lattice is simple cubic or bcc, the structure cannot be identified from the first six reflections, as the ratios of *N* values for both structures are the same. For these lattices unambigous structure determination can be carried out only if the seventh peak in the pattern is measured. If the values *N* are known for all reflections, their indices *hkl* can be obtained from Table 1. The indexing procedures for non-cubic structures are more complicated, therefore they are not applied in the laboratory exercises.

3.1.5. DETERMINATION OF LATTICE CONSTANT FOR CUBIC CRYSTALS

If the reflections of a cubic crystal are indexed, eq. (25) enables the determination of its lattice constant from the values of interplanar spacing d_{hkl} using the formula $a = d_{hkl}\sqrt{h^2 + k^2 + l^2}$. There is an experimental evidence that the lattice constants determined from the different peaks slightly deviate. This difference in the lattice constant values is due to systematic errors occurring in the determination of interplanar spacing d_{hkl}. These errors (caused e.g. by the wrong positioning of the sample) strongly depend on the Bragg-angle, yielding *hkl* dependence of the lattice constant. As the wavelength of X-ray is known with high precision, its error can be neglected. The relative error in interplanar spacing caused by the uncertainty of Bragg-angle can be expressed as:

$$\left|\frac{\Delta d_{hkl}}{d_{hkl}}\right| = \left|\cot\theta \cdot \Delta\theta\right|, \tag{26}$$

where $\Delta\theta$ is the error of Bragg-angle. Eq. (26) was obtained by differentiating the Bragg-equation. The uncertainty in the determination of the peak position usually does not change with the angle of reflection. At the same time, the absolute value of $cot\,\theta$ decreases with increasing θ in the range $0^0 < \theta < 90^0$, therefore the precision of the lattice constant value is better if it is determined from the peaks appeared at large diffraction angles. In practice, the error in the lattice parameter is eliminated by extrapolating its value to $\theta = 90^0$ using the following equation (Nelson–Riley-formula) [7]:

$$a_{hkl} = a_0 - D\cos\theta\left(ctg\,\theta + \frac{\cos\theta}{\theta}\right), \tag{27}$$

where a_{hkl} are the lattice constant values determined for the different *hkl* reflections, *D* is a constant describing the magnitude of systematic errors and a_0 is the real lattice parameter. In this analysis, the values of a_{hkl} are plotted as a function of $\cos\theta\left(ctg\theta+\frac{\cos\theta}{\theta}\right)$. The intersection of the straight line fitted to the data points with the vertical axis gives the value of a_0.

3.1.6. EVALUATION OF SOLUTE CONCENTRATION FROM LATTICE PARAMETER

In solid solution alloys, if the sizes of matrix and solute atoms differ considerably, the lattice parameter is sensitive to solute atom concentration. Thus, solute concentration can be determined by measuring the change of lattice constant relative to the lattice parameter for the pure matrix material. In this analysis, the dependence of lattice constant on solute content should be known for the studied solute-solvent atom pair. If more than two different solute atoms were dissolved in the matrix, their effects on the lattice constant may be different, therefore the solute concentration from the lattice constant can be determined only for two-component alloys. The relationship between the lattice constant and the solute concentration can be found in the literature for numerous two-component alloys (e.g. for *Al(Mg)* alloy see Ref. [8]).

4. EXERCISES

During the laboratory exercises the powder patterns are measured by a *Philips Xpert* θ-2θ diffractometer which is described in section 3.1.1 (see also Fig. 8). The studied polycrystalline sample should be placed on the sample holder, and then the voltage and the current of the diffractometer have to be increased gradually to *40 kV* and *30 mA*, respectively. In the next step, the measuring softwer (*Xpert_Data_Collector*) is started and the parameters of the measurement (starting and end 2θ angles, step size and time per step) are specified. Before we start the measurement the shutter at the X-ray tube have to be opened. The output of the software is a datafile with two columns: in the first and second columns the 2θ angle values and the counts can be found, respectively. The completion of one diffraction experiment takes 2-3 hours, therefore during the measurement former diffractograms are evaluated. In the laboratory exercises the following tasks have to be performed:

1. *Identification of an unknown crystalline phase using ICDD database.* First, the values of d_{hkl} for all measured diffraction peaks are determined according to the description given in section 3.1.2. Then, those phases are collected from the database which have the same d_{hkl} values for the three strongest peaks as for the studied sample (see section 3.1.3). Finally, from these candidates we select the phase for which the positions and the relative intensities of the weaker peaks agree well with the measured values.
2. *Determination of type of cubic lattice by indexing peaks in a powder diffraction pattern.* First, the values of d_{hkl} are determined from a diffractogram, then the indices of reflections are calculated according to section 3.1.4. Finally, the type of lattice is determined with the help of Table 1.
3. *Calculation of lattice constant and solute concentration for a metallic alloy.* First, the lattice constant is calculated from the powder pattern (see section 3.1.5). The uncertainty of 2θ is 0.01° which leads to a relative error of 10^{-4}-10^{-5} in both d_{hkl} and the lattice constant. Let's determine the solute concentration of the studied alloy from the lattice constant by the method described in section 3.1.6.

6. REFERENCES

1. B. E. Warren: X-ray diffraction, Dover Publications, New York, 1990.
2. J. Gubicza, L. Zsoldos: Röntgendiffrakció, Jegyzet a Korszerű Vizsgálati Módszerek Laboratóriumhoz (2005) in Hungarian.
3. Ch. Kittel: Introduction to Solid State Physics, John Wiley and Sons, New York, 1961.
4. H.P. Klug, L.E. Alexander: X-Ray Diffraction Procedures: For Polycrystalline and Amorphous Materials, John Wiley and Sons, New York, 1974.
5. J. Gubicza: X-ray line profile analysis in Materials Science, IGI-Global, Hershey, PA, USA, 2014.
6. http://www.icdd.com (International Centre for Diffraction Data).
7. A. Taylor: X-ray metallography, John Wiley and Sons, New York, 1961.
8. D. M. Pool, H. J. Axon: J. Inst. Met. **80** (1952) 599.